24th COBEM - 2017

24th ABCM International Congress of Mechanical Engineering
December 3-8, 2017, Curitiba, PR, Brazil

COBEM-2017-0769
COMPUTATIONAL IMPROVEMENT IN THE EVALUATION OF DYNAMIC INTEGRITY WITH MONTE CARLO METHOD

Kaio César Borges Benedetti
Frederico Martins Alves da Silva
Federal University of Goiás, av. Universitária no. 1488, 74605-220, Goiânia, Goiás.
kaio.civil@gmail.com, silvafma@ufg.br

Paulo Batista Gonçalves
Pontifical Catholic University of Rio de Janeiro, av. Marquês de São Vicente no. 225, 22451-900, Rio de Janeiro, RJ.
paulo@puc-rio.br

Abstract. *The dynamic integrity of structural systems is a modern concept in engineering analysis. It can be evaluated through the analysis of basins of attraction (BoA), a difficult task to obtain analytically. Numerical methods to find BoA have been developed in the last decades; all based on a pre-defined grid of starts (GoS) and the simple cell mapping (SCM). Since large scale systems have multiple dimensions in phase space, these methods do not scale well, being computationally cumbersome and time consuming. In this study, a new method is proposed to obtain the dynamic integrity of a structural system, based on the Monte Carlo technique. A simple mechanical system will be addressed. Through comparisons between the Monte Carlo, the GoS and SCM procedures, it is shown that the dynamic integrity measures can be estimated with minimal error and less computational processing time by the proposed method, demonstrating its effectiveness.*

Keywords: *Dynamic systems, Basin of attraction, Dynamic integrity, Monte Carlo method*

1. INTRODUCTION

The evaluation of the dynamic integrity of non-linear dynamical systems is an important problem in engineering. It can be measured by analyzing the basins of attraction (BoA), i.e., the group of initial conditions that converges to a desired attractor (Thompson, 1989). Rega and Lenci (2005) studied various one degree of freedom mechanical systems as examples, verifying that the erosion of BoAs is the primary indicator of dynamical instability, a fact already observed by Thompson (1989). Tree integrity measures were highlighted: the global integrity measure (GIM), the local integrity measure (LIM) and the integrity factor (IF), and comparisons between the GIM and IF of the investigated mechanical systems were made.

Obtaining the BoAs is not an easy task. Analytically, only some qualitative properties can be determined, making the investigation essentially a numeric one (Belardinelli and Lenci, 2016). The most basic numeric method is the grid of starts (GoS) or integration of a grid of points (IGP) or brute force method, where the phase space of initial conditions is discretized into a number of cells (Belardinelli and Lenci, 2016). Hsu (1987) formulated the simple cell mapping (SCM), checking the trajectory of each solution and reducing the computational cost. For large scale systems, calculating BoAs is computationally cumbersome, requiring the use of parallel computing (Belardinelli and Lenci, 2016).

Given a random initial condition, how likely is it to be in a given BoA? This probabilistic interpretation opens the way for a statistical analysis of integrity measures. Instead of discretizing the whole phase space, a smaller sample of initial conditions can be used to estimate the BoAs and their integrity measures, reducing the overall computational cost.

In the present work, a new procedure is proposed to evaluate the integrity measures of nonlinear dynamical systems, based on the Monte Carlo method (Shreider, 1966). To check the effectiveness of the proposed procedure, a simple dynamical system with multiple equilibrium positions, the well-known von Mises truss (Orlando, *et al*., 2016), is analyzed and the integrity measures obtained by the GoS, SCM and present method are compared in terms of precision and computation time.

2. MECHANICAL MODEL

The Von Mises truss consists of two elastic bars with elastic modulus E and cross-sectional area A. A nodal mass m is considered at the top node, along with a vertical force P. Geometric parameters l and h are considered, which define the general nonlinear behavior of the truss (Ligarò and Valvo, 2006). Figure 1 presents the reference configuration, which coincides with the tensionless case. The Lagrangian coordinate of the symmetrical case x is also represented, with zero value at the reference configuration.

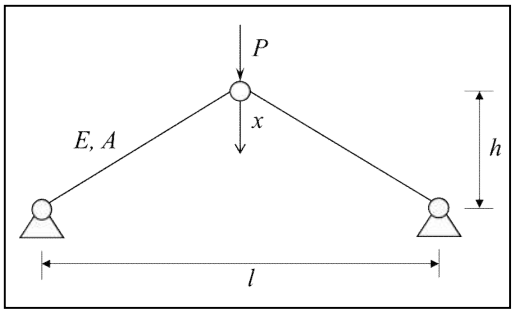

Figure 1. Von Mises truss

Considering finite strain and displacements, the Green-Lagrange strain tensor and the work-conjugate second Piola-Kirchhoff stress tensor are adopted (Ligarò and Valvo, 2006). Therefore, the axial components of strain for both bars are

$$\varepsilon = \frac{B_i^2 - B^2}{2B^2} \tag{1}$$

where the squares of the initial length B and final length B_i are

$$B^2 = h^2 + \frac{l^2}{4} \tag{2}$$

$$B_i^2 = (h - x)^2 + \frac{l^2}{4} \tag{3}$$

Using the axial components of strain defined in Eq. (1), we can write the strain energy, U, as

$$U = \frac{1}{2} EAL \sum \varepsilon^2 = EAL \left(\frac{B_i^2 - B^2}{2B^2} \right)^2 \tag{4}$$

The load potential energy V is defined as

$$V = Px \tag{5}$$

and, with Eq. (4), the total potential energy of the Von Mises truss is obtained as

$$\Pi = U - V \tag{6}$$

From Equation (6) the nonlinear equilibrium conditions is obtained by the principle of minimum potential energy, $\delta\Pi = 0$.

Taking the kinetic energy T as

$$T = \frac{1}{2} m \dot{x}^2 \tag{7}$$

the Lagrangian L is defined as the difference between the kinetic and potential energy

$$L = T - \Pi \tag{8}$$

and considering a linear viscous damping Q force given by

$$Q = 2\zeta m \omega \dot{x} \tag{9}$$

where ω is the truss natural frequency, $\dot{x}$, the velocity, m, the mass and ζ, the damping ratio, the Euler-Lagrange equation for non-conservative one degree of freedom systems is obtained

$$\frac{\partial L}{\partial x} - \frac{\mathrm{d}}{\mathrm{d}t}\left(\frac{\partial L}{\partial \dot{x}}\right) = -Q \tag{10}$$

which, in term of the system variables is, for the symmetric Von Mises truss, given by

$$m\ddot{x} + 2\zeta m\omega\dot{x} + \frac{EA}{\left(l^2 + 4h^2\right)^{0,75}}\left(16h^2 x - 24hx^2 + 8x^3\right) = P \tag{11}$$

In this paper, the following geometric parameters are considered: $l = 5$ and $h = 1$. The conservative system exhibits two homoclinic orbits around the equilibrium points $(x, \dot{x}) = (0; 0)$ and $(x, \dot{x}) = (2h; 0)$ (see Fig. 2a), indicating two competing attractors, and each one correlated to a potential well (see Fig. 2b). The left pre-buckling potential well is the desired safe region.

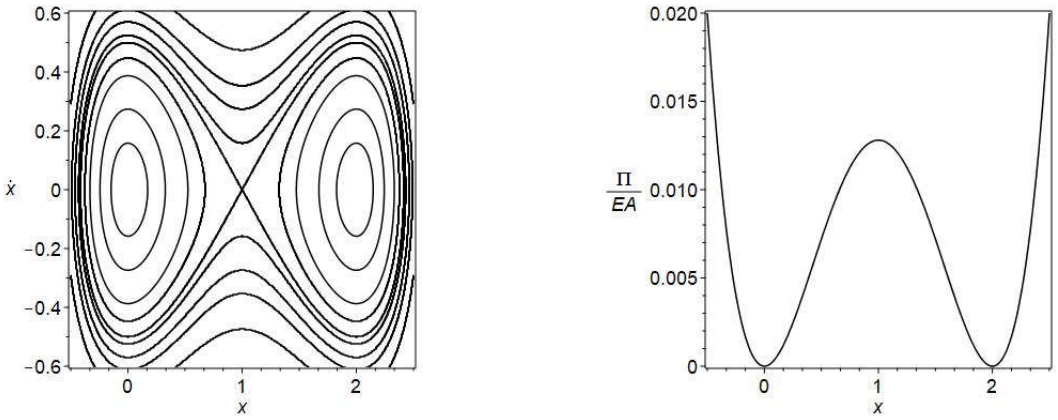

(a) (b)

Figure 2. (a) Phase portrait of the conservative system and (b) its potential energy

3. NUMERICAL RESULTS

In the following analyzes an harmonic force $P = \lambda \cos(\Omega t)$ is considered. The adopted damping ratio is $\zeta = 0{,}1$, and the time variable is normalized by the natural frequency ω, i.e., $t = \tau / \omega$. Because the natural frequency ω is a factor of $(E A / m)^{0,5}$, Eq. (11) becomes independent of E, A and m, remaining only the height h and the length l as geometric parameters and the magnitude λ and the frequency Ω as forcing parameters.

Initially the escape boundary (Thompson and Stewart, 2002) in the $(\lambda; \Omega)$ plane will be determined. For a chosen forcing frequency Ω, the bifurcation diagram of the Poincaré map (Nayfeh and Balachandran, 1995) is obtained for increasing and decreasing values of the forcing magnitude λ. Next, the dynamic integrity measures are obtained for selected values of λ, based on the analysis of the BoAs.

The Monte Carlo procedure consists in sampling a given number of initial conditions (x, $\dot{x}$) uniformly distributed in the phase-plane where they will be an estimative of the real BoA. For a large number of sampled initial conditions, the difference between the Monte Carlo procedure and the real BoA is expected to be minimal (Shreider, 1966). This estimated BoA are used to calculate the integrity measures GIM, LIM and IF, providing an estimative of these properties as well. The results of the Monte Carlo procedure are compared with those obtained by GoS and SCM procedures, evaluating its precision and the differences in processing time.

In all next results, the fourth order Runge-Kutta method is used, with time step equals 1/1000 of Ω/ω. Only the steady state is evaluated, integrating 1000 time steps to eliminate the transient state.

3.1 Dynamic stability analysis

Figure. 3a shows the permanent escape boundary for the slowly evolving system under harmonic excitation. Two large wells are noted, with $\Omega/\omega \approx 0.4$ and $\Omega/\omega \approx 0.8$, indicating regions susceptible to escape. The bifurcation diagram of the Poincaré map, for an excitation frequency of $\Omega/\omega = 0{,}4$ Fig. 3b, shows the sequence of solutions starting at each potential well. Initially only two solutions are observed, corresponding to a periodic solution at each potential well. The blue solution is within the safe pre-buckling well, while the orange solution is within the post-buckling well. A saddle-node bifurcation occurs at $\lambda/EA \approx 0{,}0134$, generating a new branch of solution, shown in green. As the amplitude increases, the initial solutions undergo saddle-node bifurcations in $\lambda/EA \approx 0{,}0173$. New solutions branches arise at the same forcing amplitude, leading to larger oscillation amplitudes. A cascade of period-doubling bifurcations occurs along both the blue and orange solutions for $\lambda/EA > 0{,}018$, resulting in chaos for $\lambda/EA > 0{,}01853$, after which both branches disappears and the green solution remains the only one in all phase-plane for a brief interval of forcing amplitude.

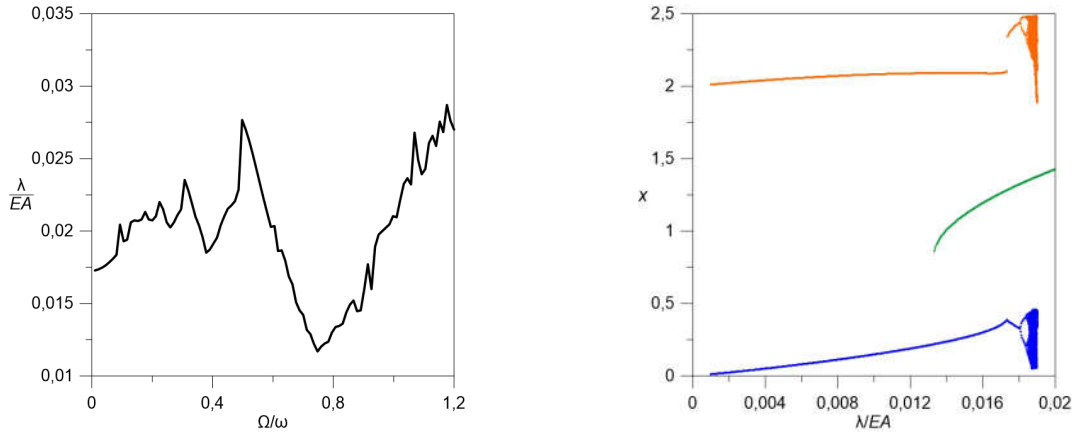

Figure 3. (a) Permanent escape boundary of the Von Mises truss and
(b) bifurcation diagram of the orbits for $\Omega/\omega = 0{,}4$

3.2 Dynamic integrity analysis

Figure 4 presents the BoAs for three forcing magnitudes λ/EA, between 0,01 and 0,0133, with forcing frequency $\Omega/\omega = 0{,}4$. They are obtained using a 500x500 GoS in the (x, $\dot{x}$) phase-plane, totalizing $2{,}5\text{x}10^5$ cells of initial conditions. The two distinct colors, blue and orange are related with the colors in the bifurcation diagram in Fig. 3b: the blue BoAs corresponds to the blue solution, while the orange BoAs corresponds to the orange solution. As the amplitude increases, the fractality along the basin boundaries increases, leading to increasing sensitivity to initial conditions. The last BoAs, for $\lambda/EA = 0{,}0133$, is extremely close to the saddle-node bifurcation that originates the green solution. The integrity measures obtained through GoS are shown in Table 1, while those obtained through SCM are presented in Table 2, for all three force magnitudes investigated in Fig. 4. Again, colors are referred to those in Fig. 4. All results are nondimensionlized with respect to the basins of the autonomous case ($P = 0$), where the safe BoA, in blue, has GIM equals to 8, LIM equals to 0,56 and IF equals to 0,664.

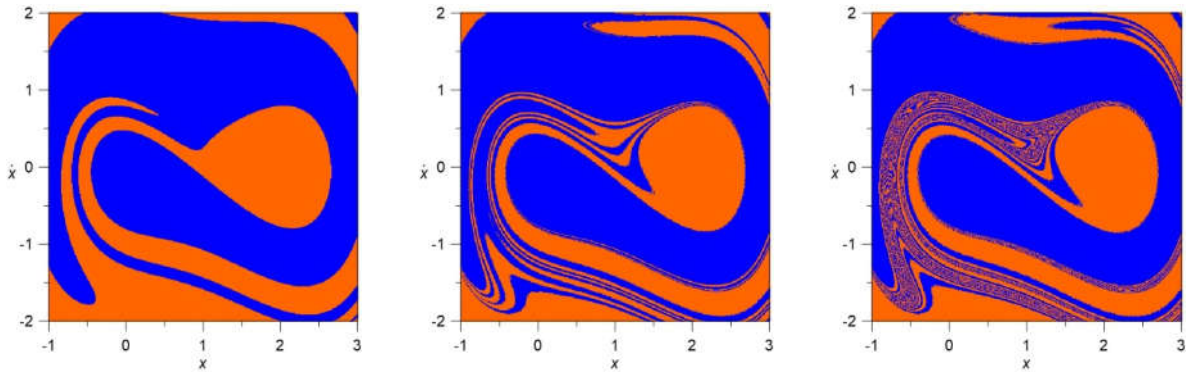

(a) $\lambda/EA = 0{,}01$ (b) $\lambda/EA = 0{,}0125$ (c) $\lambda/EA = 0{,}0133$

Figure 4. Basin of attraction obtained by de GoS method with 500x500 cells and $\Omega/\omega = 0{,}4$: (a) $\lambda/EA = 0{,}01$, (b) $\lambda/EA = 0{,}0125$, (c) $\lambda/EA = 0{,}0133$

As the amplitude increases, the three integrity measures of the pre-buckling BoA (in blue), measured using GoS method, decrease according to the GoS method (see Table 1). The GIM and LIM of the post-buckling BoA (in orange) shows an oscillatory behavior, while the IF decreases with the parameter λ/EA . The fractality effect is especially noticeable in both LIM and IF (Rega and Lenci, 2005), where sudden drops are observed from $\lambda/EA = 0{,}0125$ to $\lambda/EA = 0{,}0133$. However, because the fractality is confined to a relatively small region of the phase-plane, its influence is not so drastic.

Table 1. Integrity measures obtained by the GoS method using 500x500 cells for $\Omega/\omega = 0{,}4$, normalized with respect to the autonomous case.

λ/EA	GIM	LIM	IF
0,01	1,2347675	0,728571429	1,108433735
	0,7652325	1,057142857	1,072289157
0,0125	1,26098375	0,614285714	0,843373494
	0,73901625	1,085714286	0,987951807
0,0133	1,2148475	0,557142857	0,819277108
	0,7851525	0,971428571	0,939759036

The SCM method results differ from those obtained using the GoS method (see Table 2). This difference is caused by the increasing propagating errors in the SCM process (Hsu, 1987). The GIMs are particularly susceptible to this effect, as observed in the discrepancy between the values of Table 1 and Table 2. For these reasons, the Monte Carlo procedure will be compared to the GoS method alone, since this method, when a suitably high number of cells is used, is the closest approximation to the BoAs correct result.

Table 2. Integrity measures obtained by the SCM method using 500x500 cells for $\Omega/\omega = 0{,}4$, normalized with respect to the autonomous case

λ/EA	GIM	LIM	IF
0,01	1,2325125	0,728571429	1,072289157
	0,7674875	1,057142857	1,072289157
0,0125	1,2736	0,6	0,855421687
	0,7264	1,085714286	0,987951807
0,0133	1,30974375	0,557142857	0,819277108
	0,69025625	0,971428571	0,939759036

Figures 5 to 7 contain the errors in the three integrity measures obtained by the proposed Monte Carlo procedure with respect to the GoS results shown in Table 1, as well as the total processing time, i.e., the processing time necessary to calculate the BoAs plus all the integrity measures of the two competing solutions, of all methods, for three load levels illustrated in Fig. 4. These errors and processing times of the Monte Carlo procedure are evaluated as a function of increasing number of sample, from 1% to 10% of the total number of cells used in the GoS method ($2{,}5 \times 10^5$ cells). The

cells are sampled randomly, filtering those already sampled. For that reason, the sample sizes are slightly smaller than the initial percentage value. Two error measures are

$$\text{Percentage error} = \frac{|V_{GoS} - V_{MC}|}{V_{GoS}} \cdot 100\% \tag{12}$$

$$\text{Absolute error} = |V_{GoS} - V_{MC}| \tag{13}$$

where V_{GoS} consists of the values given in Table 1, while V_{MC} is the result obtained by the Monte Carlo procedure.

The error of the GIM decreases with the sample size for all force magnitudes and all BoAs. This fact is expected because the BoAs' fractality is restricted to small regions of the phase-plane. Being the GIM a measure of the global area of a given BoA (Rega and Lenci, 2005), the error is proportional to $1/\sqrt{N}$, being N the sample size (Shreider 1966). For a small sample of around 5000 cells, the percentage errors are less than 1% in all cases. In addition, the comparatively small processing time observed in Figs. 5c, 6c and 7c demonstrates that the Monte Carlo procedure is a reliable method for the evaluation of dynamical integrity measure, with minimal loss of precision.

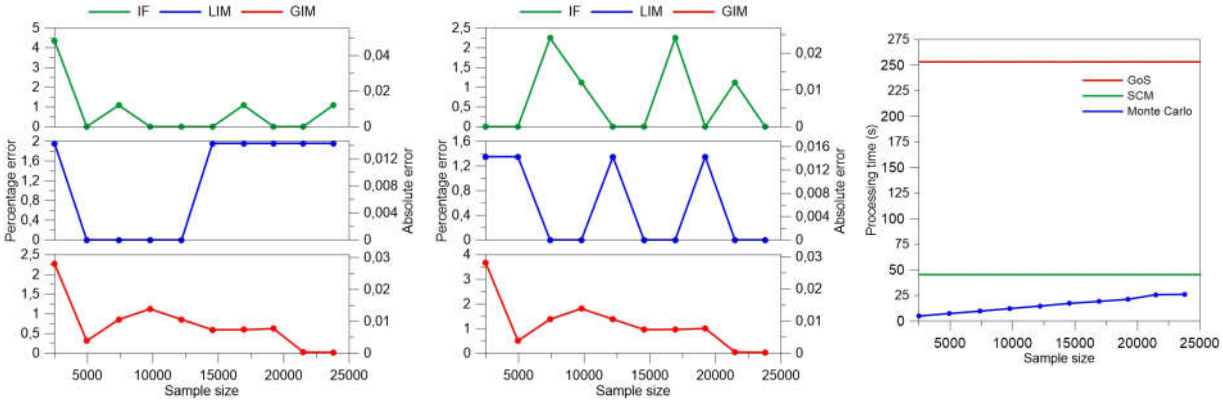

(a) *blue basin* (b) *orange basin* (c) processing time

Figure 5. Integrity measures' error progression obtained with Monte Carlo for $\Omega/\omega = 0{,}4$ and $\lambda/EA = 0{,}01$: (a) blue basin, (b) orange basin and (c) total processing time

The LIMs error oscillates with the sample size, especially in Figs 5a and 5b. The increasing percentage error with the force magnitude for small samples is another noticeable fact. Table 1 shows that the LIM values of the blue basin decrease with the force magnitude, indicating that the attractor approaches the basin boundary. An apparent conclusion is that, for small integrity values, a bigger sample is necessary for a good estimation from the Monte Carlo procedure. Nevertheless, the absolute errors, for all cases and BoAs, are of the order of 10^{-2}, for all sample sizes, with much smaller processing time.

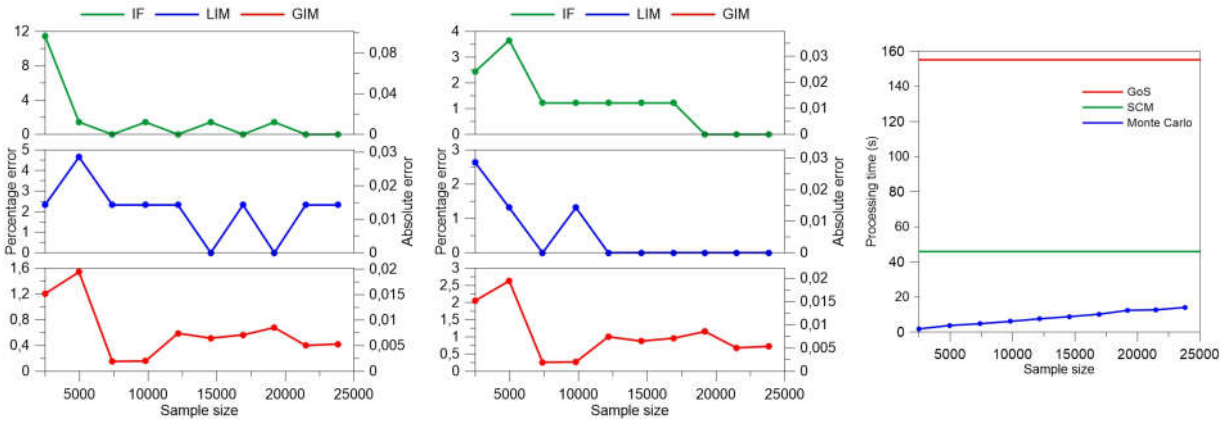

(a) blue basin (b) orange basin (c) processing time

Figure 6. Integrity measures' error progression obtained with Monte Carlo for $\Omega/\omega = 0{,}4$ and $\lambda/EA = 0{,}0125$: (a) blue basin, (b) orange basin and (c) total processing time

The IFs, similar to the LIMs, oscillate with the sample size. However, the percentage errors are always less than 4% even for sample sizes as small as 5000 cells, which is a good indication that the Monte Carlo procedure can be used as an estimator of the IF of a desired solution. The absolute error is of order of 10^{-2} for all sample sizes.

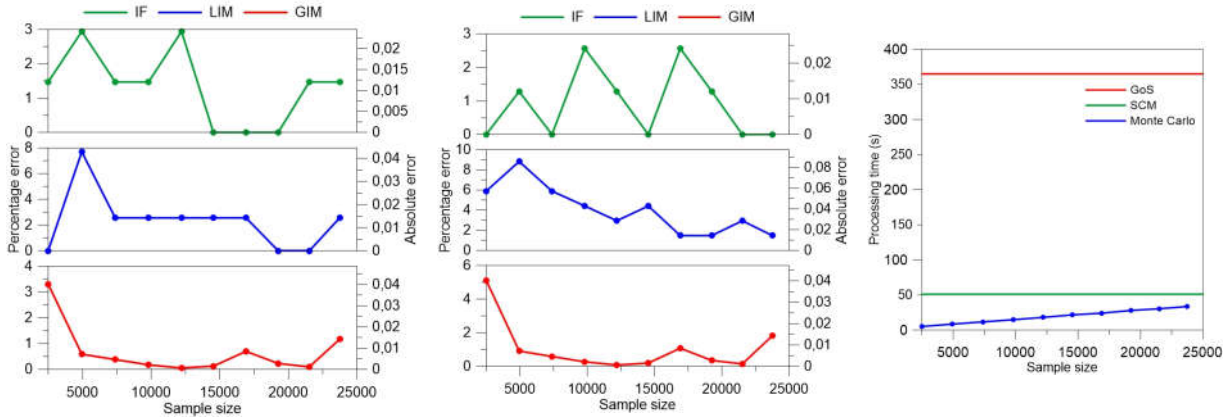

(a) $x \approx 0$ (b) $x \approx 2$ (c) processing time

Figure 7. Integrity measures' error progression obtained with Monte Carlo for $\Omega/\omega = 0{,}4$ and $\lambda/EA = 0{,}0133$: (a) blue basin, (b) orange basin and (c) total processing time

4. CONCLUDING REMARKS

In the present work, a procedure for estimating the integrity measures of the basins of attraction of nonlinear dynamical systems with competing attractors is proposed. For comparison purposes, a single degree of freedom mechanical model displaying multiple attractors and dynamic instabilities has been chosen. Three integrity measures have been evaluated (the global integrity measure (GIM), the local integrity measure (LIM) and the integrity factor (IF)) through three methods: (1) the brute force method based on a pre-defined grid of starts (GoS), (2) the simple cell mapping (SCM) and (3) the proposed method based on the Monte Carlo approach, for three distinct forcing magnitudes. An analysis of the error and computation time of the present method was compared with those obtained by the other methods. In general, a sample of 2% of the cells used in the other two methods can be used to estimate the integrity measures with small errors, leading to a much smaller processing time. However, it is necessary to verify the statistical properties of the proposed Monte Carlo procedure in order to establish a security interval of the estimated integrity measures. There is also space for computational improvement of the Monte Carlo procedure, especially in the sampling step, in order to eliminate the filter.

5. ACKNOWLEDGEMENTS

This work was made possible by the support of the Brazilian Ministry of Education, CAPES, CNPq, FAPERJ-CNE and FAPEG.

6. REFERENCES

Belardinelli, P. and Lenci, S., 2016. "An Efficient Parallel Implementation of Cell Mapping Methods for MDOF Systems." *Nonlinear Dynamics*, Vol. 86, Is. 4, p. 2279–2290.

Hsu, C.S., 1987. *Cell-to-Cell Mapping*. Springer New York, New York, NY, 1st edition.

Ligarò, S.S. and Valvo, P.S., 2006. "Large Displacement Analysis of Elastic Pyramidal Trusses." *International Journal of Solids and Structures*, Vol. 43, Is. 16, p. 4867–4887.

Nayfeh, Ali H. and Balachandran, B., 1995. *Applied Nonlinear Dynamics: Analytical, Computational, and Experimental Methods*. Wiley, New York, NY, 1st edition.

Orlando, D., Gonçalves, P.B., Lenci, S. and Rega, G., 2016. "Increasing Practical Safety of Von Mises Truss via Control of Dynamic Escape." *Applied Mechanics and Materials*, Vol. 849, p. 46–56.

Rega, G. and Lenci, S., 2005. "Identifying, Evaluating, and Controlling Dynamical Integrity Measures in Non-Linear Mechanical Oscillators." *Nonlinear Analysis: Theory, Methods & Applications*, Vol. 63, Is. 5–7, p. 902–914.

Shreider, Yu. A., 1966. "Principles of the Monte Carlo Method." p. 1–90 in *The Monte Carlo Method*, edited by Y. A. Shreider. Pergamon, 1st edition.

Thompson, J.M.T., 1989. "Chaotic Phenomena Triggering the Escape from a Potential Well." *Proceedings of the Royal Society A: Mathematical, Physical and Engineering Sciences*, Vol. 421, Is. 1861, p. 195–225.
Thompson, J.M.T. and Stewart, H.B., 2002. *Nonlinear Dynamics and Chaos*. Wiley, Chichester, England, 2nd edition.

7. RESPONSIBILITY NOTICE

The authors are the only responsible for the printed material included in this paper.